# Quench Protection of the 16 T $Nb_3Sn$ Dipole Magnets Designed for the Future Circular Collider

T. Salmi, M. Prioli, A. Stenvall, and A. P. Verweij

***Abstract*—Three different 16 T dipole magnet options for the Future Circular Collider (FCC) have been designed within the H2020 EuroCirCol collaboration, namely a cosθ-, a block- , and a common-coil -type of magnet. All magnets were designed using the same constraints related to magnetic field, cable parameters, mechanics, and quench protection. The quench protection analysis during the magnet design was centralized and done for all the options using the same tools and methods. This paper summarizes the final conceptual protection schemes. They are based either on the novel CLIQ-technology (Coupling Loss Induced Quench) or on traditional quench heaters. We compare the performance of the protection systems and show that while both can protect the magnet at nominal operation current, CLIQ is more efficient in reducing peak temperatures than heaters, and the system operation is simpler due to smaller amount of protection units. Therefore, CLIQ has been chosen as the baseline protection option for the FCC dipole magnets. The future development of heaters is considered as a back-up option.**

***Index Terms*— Future Circular Collider, FCC, particle accelerators, superconducting magnets, quench protection**

## I. Introduction

PARTICLE accelerators are instruments which allow high-energy physics research probing deeper to the unknown 95% of the matter in universe, and strengthening our understanding of the known material territory. The international particle accelerator community is presently looking to the future, and finalizing the preparation of a conceptual design report (CDR) of the technologies needed for a 100 km long, 100 TeV hadron-hadron collider allowing the next generation high-energy physics research. This Future Circular Collider (FCC) study is a CERN coordinated, five-year effort including institutes from 34 countries. The post-LHC synchrotron, with the working title FCC, is foreseen to be operational around 2040, and to be based on highly challenging superconducting 16 T $Nb_3Sn$ dipole magnets. [1]-[3]

The conceptual design of the FCC dipole magnets was done within the EU H2020 funded European Circular Energy-Frontier Collider Study (EuroCirCol) collaboration [4]-[7]. Three conceptually different 16 T dipole magnet options were analyzed, and successfully designed. A cosθ-type magnet [8], [9] was designed at the National Institute of Nuclear Physics (INFN) in Milan and Genoa, Italy, a block-type magnet [10], [11] at the French Alternative Energies and Atomic Energy Commission (CEA) in Saclay, France, and a common-coil -type magnet [12] at the Research Centre for Energy, Environment and Technology (CIEMAT) in Madrid, Spain. All the magnet options were based on the same design parameter space, discussed in [5]-[7]. One of the critical aspects in the magnet design was their protection in case of a quench, i.e., a sudden loss of superconductivity within the windings [13]. In order to ensure that the magnets can be protected, the quench protection was considered from the very beginning of the magnet design [14]. The protection studies were performed by Tampere University of Technology (TUT) and CERN.

It was set as a design criterion that if a magnet quenches at 105% of the nominal operation current, the hotspot temperature must stay below 350 K. This calculation was based on an estimated efficiency of the potential quench protection system. The efficiency was defined as so-called protection delay, composed of the time needed to detect and validate the quench (20 ms) and the time required to effectively quench the entire winding (20 ms). In other words, the magnet designs must have a so-called 40 ms time margin to 350 K [15]. Detailed discussion on the methods can be found in [14-16]. Fast-feedback tools were provided to magnet designers to verify the temperature criterion, and the detailed temperature and voltage distributions were computed adiabatically with the software Coodi [14],[17].

As the magnet designs matured, conceptual protection designs based on the Coupling Loss Induced Quench (CLIQ) system and quench heaters (QH) were developed for each magnet design option. QH are a conventional technology, based on resistive strip heaters on coil surfaces which upon quench detection are powered with a capacitor discharge. Up to now, the quench protection of high-current accelerator magnets has been based on QH [18]-[20]. On the other hand, CLIQ is a novel technology developed at CERN and the HL-LHC (High Luminosity LHC) collaboration during the recent years, and will be implemented in the HL-LHC inner triplet alongside with QH [21],[22]. It is based on the discharge of a capacitor across part of the windings. The changing current and magnetic field induce inter-filament and inter-strand coupling losses which rapidly quench a large fraction of the superconducting coil. Simulations and measurements on the LHC and HL-LHC magnets

T. Salmi, and A. Stenvall are with Tampere University, FI-33014 Tampere University, Finland (e-mail : tiina.salmi@tut.fi), [2]M. Prioli was with CERN and is now with INFN, 20133 Milano, Italy, [3]A. P. Verweij is with CERN.

Manuscript received 26th October 2018.

This work was supported by the Academy of Finland (QuenchCirCol, Grant 295185), and by the European Union's Horizon 2020 research and innovation programme under Grant 654305, EuroCirCol project.

Color versions of one or more of the figures in this paper are available online at http://ieeexplore.ieee.org.

Digital Object Identifier will be inserted here upon acceptance.

have indicated that CLIQ is more efficient in quenching the coils and reducing hotspot temperature than QH [22]-[25].

In this paper we summarize the quench protection designs for the FCC 16 T dipole magnets, and compare the performance of the CLIQ and QH systems in terms of maximum temperatures, voltages, and complexity of the system. The focus is on single magnets. Protection of the entire circuit is analyzed in [26].

## II. The Magnet Designs

The 16 T $Nb_3Sn$ dipole magnet designs considered in these studies are very similar to those put in the CDR, and the results given in this paper can therefore be considered representative. The magnet parameters relevant for the protection studies are summarized in Table I. In addition, the magnetic field maps from ROXIE [27] are used. All magnets are 14.3 m long, double-aperture designs operating at 1.9 K. The cable insulation is 0.15 mm thick impregnated glass, the Cu RRR is assumed to be 100, and the filament twist pitch 14 mm. The G10 insulation between the coil layers is 0.5 mm thick. The coils are graded, having a smaller cable at the low-field (LF) region, and a larger at the high-field (HF) region to save on conductor quantity and to balance the quench margins within the coil regions.

TABLE I
Magnet parameters used in the simulations.

| | Cosθ [5] | Block [6] | C-c [7] |
|---|---|---|---|
| Reference version | v22b-38-v1 | V5ari204 | vh12_2ac6 |
| Nominal current, $I_{nom}$ (A) | 11390 | 10111 | 16400 |
| Inductance @$I_{nom}$ (mH/m/2-ap.) | 39.6 | 49.6 | 21.1 |
| Cable width (HF / LF) (mm) | 13.2/ 14.0 | 12.6 / 12.6 | 19.2 / 12.0 |
| Cable thickness (HF/ LF) (mm) | 1.89/ 1.20 | 2.00 / 1.27 | 2.20 / 2.20 |
| Number of strands (HF / LF) | 22 / 38 | 21 / 34 | 30 / 18 |
| Strand diam. (HF / LF) (mm) | 1.1 / 0.7 | 1.1 / 0.7 | 1.2 / 1.2 |
| Strand Cu /$Nb_3Sn$ (HF / LF) | 0.82 / 2.1 | 0.8 / 2.0 | 1.0 / 2.5 |

The simulations assume the FCC target $Nb_3Sn$ critical current density (2300 A/mm² @ 1.9 K and 16 T), and the Bordini parameterization as a function of magnetic field and temperature [28]. The simulated $Nb_3Sn$ specific heat capacity is based on [29] above 20 K, and on [30] below 20 K. Other material properties are based on NIST data [31]. Only interfilament coupling currents were considered in the simulation.

## III. Protection Design Goals and Methods

The protection system design has to meet two requirements. First, the increase of the coil resistance has to be fast enough to drive a current decay such that the hotspot temperature stays below the specified limit of 350 K [14],[32]. Second, the resistance development in the windings must be such that the inductive and resistive voltages are distributed in a balanced way so that the potential to ground does not exceed the limit of 1.2 kV anywhere in the coil in nominal operation [6]. Furthermore, the design aims at minimizing the complexity of the protection systems.

The current decay rate reaches values in the order of 70 kA/s, and for a 14 m long magnet with an inductance in the order of 20 mH/m per aperture, the maximum total inductive voltage is in the order of 20 kV per aperture. The inductive voltage across each coil turn depends on the mutual inductance with the rest of the coil, and typically the turns with lower magnetic fields see higher inductive voltage. In a single magnet by-passed with a diode the sum of the resistive voltage equals the inductive voltage, but both voltages are not distributed proportionally, thus voltage differences occur inside the coils. Distributions of inductive and resistive voltages were shown in [14] considering earlier versions of the magnets.

In graded coils, the resistance of the HF cables tends to be lower than in the LF cables, which helps in balancing the voltages. On the other hand, in order to obtain a sufficient resistance increase, it is important to quench quickly the LF-cable. The LF-cable subject to the highest field develops the highest temperatures, and participates strongest to the resistance increase.

## IV. Baseline: Protection with CLIQ

The final CLIQ designs were done using the software STEAM-LEDET [33]-[34] and STEAM-COSIM with PSPICE and LEDET [34]-[36] co-simulation. The CLIQ designs were done jointly by CERN and TUT. The final simulations for the two aperture magnets were done at CERN using the software COMSOL and exploiting the STEAM-SIGMA model builder [34]-[36]. The detailed results of the final CLIQ simulations are presented in [37]. Here we summarize the designs and the aspects relevant for comparison with quench heaters.

Fig. 1 shows the connections of the CLIQ units to the windings of each magnet. The locations of the dissipated losses are indicated based on the LEDET simulations. The simulated peak temperatures and voltages at nominal current are summarized in Section VI. Each CLIQ design is able to quench the magnet also at 1 kA ensuring the protection at lower currents.

### A. *Cosθ design*

The four-layer graded cosθ dipole magnet can be protected with one CLIQ unit per aperture. It can be connected between the 3rd and 4th layer of the dipole such that the largest magnetic field change rate and coupling loss occur in those layers in both coils. This configuration quenches effectively the LF cable for rapid resistance increase and the low field turns for favorable internal voltage distribution. The CLIQ unit has 1.25 kV voltage, and 50 mF capacitance.

### B. *Block design*

In the block dipole magnet two CLIQ units per aperture are needed. The LF cables are distributed in all the four coil layers and one CLIQ unit cannot quench them all fast enough. The coil winding order and the CLIQ unit voltages are optimized for reducing the ground voltage build-up. The CLIQ unit connected between the first and the second layer has higher stored energy than the one between the two upper coil layers (CLIQ2: 1.2 kV, 50 mF vs. CLIQ1: 0.6 kV, 50 mF).

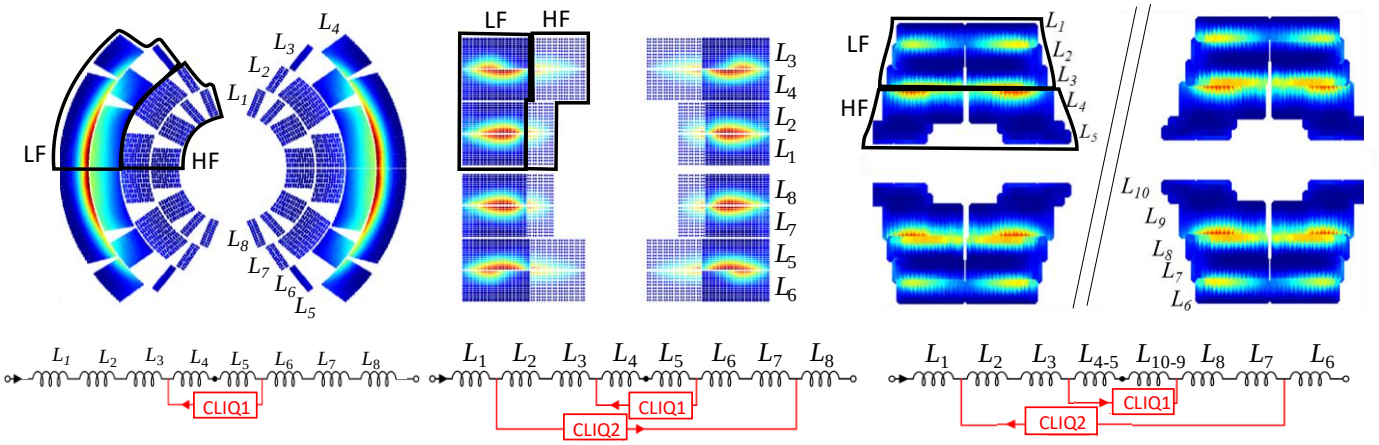


Figure 1: CLIQ connection schemes in a) cosθ, b) block, and c) common-coil type magnets. The location of largest deposited coupling losses is shown in red.

### C. *Common-coil design*

Like in the block magnet, the common-coil magnet cannot be protected with a single CLIQ unit. However, two units for two apertures can be connected in a very efficient way, and the resulting quick current change quenches the magnet very fast. The losses are also deposited in the low field region which helps in the voltage distribution. The challenge is that the layers include many turns, and the voltage build-up within one layer can be significant.

## V. Back-up Solution: Protection with Heaters

The quench heaters are assumed to be based on a similar trace technology as implemented in the HL-LHC magnets. The heaters are 25 µm thick stainless steel strip heaters glued on a 75 µm thick polyimide. The polyimide thickness is larger compared to the 50 µm in HL-LHC magnets. The stainless steel is further copper cladded to provide so-called heating stations (HS) and reduce the voltage across the strip [38]. The traces are placed on coil surfaces after the heat treatment, and impregnated together with the coils.

The heater strips are connected in circuits, and powered with a capacitor bank unit, containing a 10 mF capacitor charged to 1.2 kV. We assume that the wires connected to each circuit have a 1 Ω resistance in series with the capacitor. Each strip is U-shaped and 2x14.3 m long (Fig. 2).

The heater delays, i.e., the times to quench the cables after heater activation, were simulated for each turn using the 2-D heat diffusion model CoHDA [39] and the delays were then taken as input for the adiabatic Coodi simulation. It was assumed that the quench propagation speed between heating stations is 20 m/s, and the turn-to-turn quench delay is 10 ms. Heater design and simulations were done by TUT.

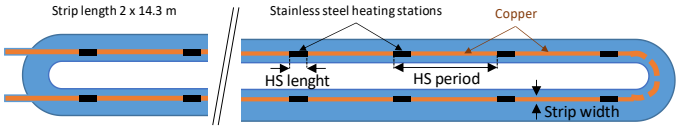


Figure 2: Schematic of copper plated heater strips on a coil surface. The heater provokes quenches under the heating stations, and the quench naturally propagates between them.

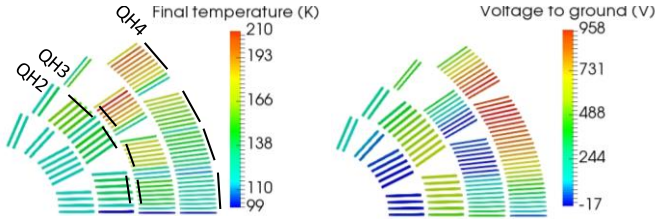


Figure 3: The location of the heater strips for the cosθ design and the maximum temperature and voltage after the heater activation.

### A. *Cosθ design*

The cosθ design has two separately impregnated two-layer-coils and it is assumed that heaters can be placed on the surface of each. However, heaters are not fixed to the unsupported innermost surface since there they may be prone to detachment [40].

The approximate locations of the heater strips onto the coil surfaces are shown in Fig. 3. The heaters covering the 2nd and 3rd layer (QH2-3) are 1 cm wide and have 4 cm long heating stations with an 18 cm period. Four strips are powered in parallel, so that the peak power ($P_{QH,t=0}$) is 100 W/cm$^2$ and circuit RC time constant ($\tau_{RC}$) is 40 ms. The heater strips on the 4th layer (QH4) need higher power and longer heating segments due to the lower magnetic field and larger energy margin. They are 1.3 cm wide with 6 cm long heating stations with a 30 cm period. Powering two strips in parallel gives $P_{QH,t=0}$=150 W/cm$^2$ and $\tau_{RC}$=50 ms. For a double-aperture magnet 14 capacitor banks are needed.

### B. Block design

Heaters can be placed on all the coil surfaces of the block coils since also the mid-plane is supported. Fig. 4 shows the approximate location of the heater strips, and the temperature and voltage distribution after the heater activation. The details of strip geometry and powering are shown in Table II.

### C. Common-coil design

In the common-coil the resistance needs to grow in layers covered by QH2-4 (see fig. 5). The strip locations are presented in Fig. 5 and their geometry and powering in Table II.

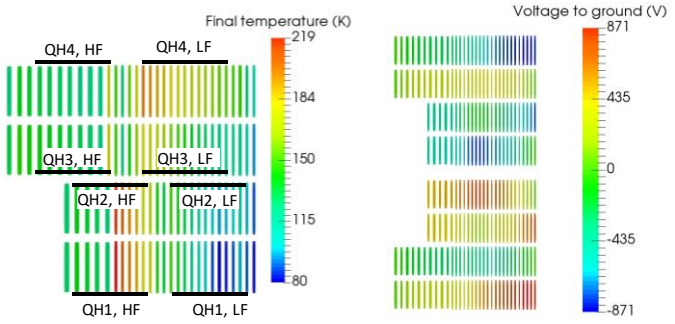


Figure 4: The location of the heater strips for the block design and the maximum temperature and voltage after the heater activation.

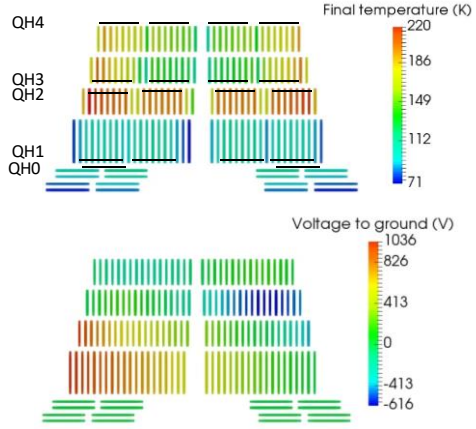


Figure 5: The location of the heater strips for the common-coil design and the maximum temperature and voltage after the heater activation.

TABLE II
HEATER STRIP GEOMETRY AND POWERING CIRCUITS

| QH | $N_{strips,}$ in par. | $w_{strips}$ (cm) | *HS/per.* (cm) | $P_{QH,t=0}$ (W/cm$^2$) | $\tau_{RC}$ (ms) |
|---|---|---|---|---|---|
| | | Cosθ | | | |
| QH2-3 | 4 | 1 | 4/18 | 100 | 40 |
| QH4 | 2 | 1.3 | 6/30 | 150 | 50 |
| | | Block | | | |
| QH1-2 HF | 2 | 1.9 | 5/22 | 100 | 40 |
| QH1-2 LF | 2 | 1.8 | 6/30 | 130 | 40 |
| QH3-4 HF | * | 2.1 | 5/35 | 100 | 20 |
| QH3-4 LF | 2 | 2.4 | 6/30 | 110 | 30 |
| | | Common-coil | | | |
| QH0-1 | 4 | 1.5 | 4/19 | 90 | 30 |
| QH2-4 | 2 | 1.75 | 6/31 | 140 | 40 |

* 2 strips in series, in parallel with the other 2-strip-set

## VI. Discussion and Comparisons

### A. Peak temperatures and voltages

The simulated hotspot temperatures and voltages to ground as well as the number of protection units are summarized in Table III for each protection method. Quench detection and validation delay is assumed to be 20 ms. In CLIQ simulations an additional 1 ms switch delay is added.

TABLE III
SIMULATED PEAK TEMPERATURES AND VOLTAGES AT NOMINAL CURRENT

| | $T_{Hotspot}$ (K) | | $V_{gnd}$ (V) | | $N_{Units/magnet}$ | |
|---|---|---|---|---|---|---|
| | CLIQ | QH | CLIQ | QH | CLIQ | QH |
| Cosθ | 286 | 322 | 800 | 870 | 2 | 14 |
| Block | 281 | 321 | 730 | 870 | 4 | 13 |
| C-c | 284 | 330 | 1100 | 1040 | 2 | 15 |

The heaters allow for well-known location of heat deposition, and profit from the natural quench propagation between the heating stations. However, due to the time associated with thermal diffusion through the heater insulation, the delay times are so long that the total resistance will not increase fast enough if low-field area is quenched before high-field area.

The peak temperatures obtained with the CLIQ based protection are significantly lower than with the heaters: 280-290 K with CLIQ vs. 320-330 K with QH. At 5% above the nominal current, the peak temperatures reach 350 K with heaters, while with CLIQ they are 40-50 K lower. The expected uncertainty in the simulation results is in the order of 20 K.

The peak voltages for both protection methods do not differ significantly, and can be considered to be within the simulation uncertainty, estimated to be 100-300 V.

### B. System complexity and redundancy

In addition of the lower peak temperature, a definite advantage to CLIQ is the smaller amount of protection units, namely maximum 4 units per double-aperture magnet, while with heaters up to 15 units are needed. On the other hand, the CLIQ units are significantly more complex and expensive, as it is required that the redundancy in all component failure cases is built internally to the unit.

With heaters the system gets complex due to the large number of powering units, but also due the large number of heater strips. To obtain sufficient redundancy to survive failures in the system requires adding even more powering units. However, the system is not very sensitive to losing an individual strip: A failure analysis in which 1 strip was disconnected symmetrically in all coils increased the temperature less than 5 K.

## I. Conclusions

Quench protection requirements were accounted in the design of the three different 16 T dipole magnets, which were developed by the EuroCirCol collaboration. The conceptual quench protection system designs are based either the CLIQ system or quench protection heaters. Based on simulations, both systems could protect each magnet at nominal current,

keeping the peak temperatures below 350 K and voltages below 1.2 kV. CLIQ was more efficient since the hotspot temperatures were about 40 K lower. Moreover, the need of heater strips and heater powering capacitor banks was fairly high: 13-15 capacitor banks for each double aperture magnet, depending on the magnet design. With CLIQ 2-4 units were sufficient.

CLIQ based protection was chosen as a baseline for the magnets. Although potentially more complex, heater based protection is considered as a back-up solution should there rise any unforeseen issue with the novel CLIQ technology in an accelerator environment.

## ACKNOWLEDGMENT

The presented work was done in close collaboration with EuroCirCol WP5 magnet designers and coordinators, and the CERN TE-MPE-PE STEAM team.

## REFERENCES

[1] Future Circular Collider Study. Website: https://fcc.web.cern.ch/Pages/default.aspx, Accessed on: Sep 28, 2018.

[2] F. Zimmermann, "Accelerators in the 21st Century", *EPJ Web of Conferences* 182, 02134, 2018.

[3] M. Benedikt and Frank Zimmermann, "Towards future circular colliders", *Journal of the Korean Physical Society* 69, 893, 2016.

[4] EuroCirCol – The European Circular Energy-Frontier Collider Study. Website: https://fcc.web.cern.ch/eurocircol/Pages/default.aspx, Accessed on: Sep 28, 2018.

[5] D. Tommasini, et al., "Status of the 16 T dipole development program for a future hadron collider", *IEEE Trans. Appl. Supercond.*, 28 3, 4001305, 2018.

[6] D. Tommasini et al., "The 16 T Dipole Development Program for FCC", *IEEE Trans. Appl. Supercond.*, 27 4, 4000405, 2017.

[7] D. Schoerling et al., "The 16 T Dipole Development Program for FCC and HE-LHC", submitted to *IEEE Trans. Appl. Supercond.*

[8] V. Marinozzi et al., "Conceptual Design of a 16 T cos θ Bending Dipole for the Future Circular Collider *IEEE Trans. Appl. Supercond.*, 28 3, 4004205, 2018.

[9] R. Valente et al. "Baseline Design of a 16 T cos θ Bending Dipole for the Future Circular Collider", submitted to *IEEE Trans. Appl. Supercond.*

[10] C. Lorin et al., "Design of a $Nb_3Sn$ 16 T Block Dipole for the Future Circular Collider", *IEEE Trans. Appl. Supercond.*, 28 3, 4005005, 2018.

[11] M. Segreti et al., 2D and 3D Design of the Block-coil Dipole Option for the Future Circular Collider, submitted to *IEEE Trans. Appl. Supercond.*

[12] F. Toral et al., "Magnetic and mechanical design of a 16 T common coil dipole for FCC", *IEEE Trans. Appl. Supercond.*, 28 3, 4004305, 2018.

[13] M. Benedikt et al., "Challenges for highest energy circular colliders", Proc. IPAC Int. Conf. Accelerators 2014, and CERN-ACC-2014-0153, 2014.

[14] T. Salmi, et al., "Quench protection analysis integrated in the design of dipoles for the Future Circular Collider", *Physical Review Accelerators and Beams* 20 3, 032401, 2017.

[15] E. Todesco, "Quench limits in the next generation of magnets," in Proc., WAMSDO 2013, CERN Geneva, Switzerland, 15-16 Jan 2013

[16] T. Salmi and D. Schoerling, "Energy density-method: An approach for a quick estimation of quench temperatures in high-field accelerator magnets", accepted for publication in *IEEE Trans. Appl. Supercond.*

[17] T. Salmi and A. Stenvall, "The Impact of Protection Heater Delays Distribution on the Hotspot Temperature in a High-Field Accelerator Magnet," *IEEE Trans. Appl. Supercond.*, 26 4, 2016.

[18] R. Stiening et al.,"A superconducting synchrotron power supply and quench protection scheme", *IEEE Trans. On Magn.*, 15, 670, 1979.

[19] F. Rodriguez-Mateos and F. Sonnemann, "Quench heater studies for the LHC magnets", Proceedings of PAC 2001, 3451, 2001.

[20] S. Izquierdo-Bermudez, *et al.*," Quench Protection of the 11 T $Nb_3Sn$ Dipole for the High Luminosity LHC" *IEEE Trans. Appl. Supercond.*, 28 3, 4006405, 2018.

[21] E. Ravaioli, CLIQ: A new quench protection technology for superconducting magnets, Ph.D. thesis, University Twente and CERN, 2015

[22] P. Ferracin et al., "Development of MQXF: The $Nb_3Sn$ low-β quadrupole for the HiLumi LHC," *IEEE Trans. Appl. Supercond.*, 26 4, 4000207, 2016.

[23] E. Ravaioli et al., "Quench Protection Performance Measurements in the First MQXF Magnet Models", *IEEE Trans.Appl.Supercond.*, 28 3, 4701606, 2018.

[24] E. Ravaioli et al., "First implementation of the CLIQ quench protection system on a full-scale accelerator quadrupole magnet", *IEEE Trans.Appl.Supercond.*, 26, 2016.

[25] E. Ravaioli et al., "First implementation of the CLIQ quench protection system on a 14 m long full-scale LHC dipole magnet", *IEEE Trans.Appl.Supercond.*, 26, 2016.

[26] M. Prioli, et al., "Design and protection of FCC-hh dipole circuits", to be published.

[27] S. Russenschuck, "ROXIE : A Computer Code for the Integrated Design of Accelerator Magnets," 6th Eur. Part. Accel. Conf. Stock. Sweden; Cern., pp. 2017–2019, Feb. 1999.

[28] F. Toral and D. Tommasini, Eds., "16 T dipole design options: Input parameters and evaluation criteria," EuroCirCol, Geneva, Project Note, EuroCirCol-P1-WP5-Note-160624, 2016.

[29] G. S. Knapp, et al., "Phonon properties of *A*-15 superconductors obtained from heat-capacity measurements", *Phys. Rev. B* 13, 3783–3789, 1976

[30] L. Dresner, "Stability of superconductors", Plenum, 1995

[31] NIST - E.D. Marquardt et al., "Cryogenic material properties database", in Proc. 11th Int. Cryocooler Conf., Keystone, 2000, http://cryogenics.nist.gov/MPropsMAY/material%20properties.htm

[32] G. Ambrosio, "Maximum allowable temperature during quench in Nb3Sn accelerator magnets," in Proc., WAMSDO 2013, CERN Geneva, Switzerland, 15-16 Jan 2013.

[33] E. Ravaioli, B. Auchmann, M. Maciejewski, H. ten Kate, and A. Verweij, "Lumped-element dynamic electro-thermal model of a superconducting magnet," *Cryogenics*, 2016.

[34] STEAM: Simulation of Transient Effects in Accelerator Magnets. Website: https://espace.cern.ch/steam/, Accessed on Sep 28, 2018)

[35] L. Bortot, et al., "A Consistent Simulation of Electro-Thermal Transients in Accelerator Circuits", *IEEE Trans. Appl. Supercond.*, 27 4, 2017.

[36] L. Bortot, et al., "STEAM: A Hierarchical Cosimulation Framework for Superconducting Accelerator Magnet Circuits, *IEEE Trans. Appl. Supercond.*, 28 3, 4900706, 2018.

[37] M.Prioli, "The CLIQ quench protection system applied to the FCC-hh dipole magnets", *to be published*

[38] H. Felice *et al*., "Instrumentation and quench protection for LARP $Nb_3Sn$ magnets," *IEEE Trans. Appl. Supercond.*, 19 3, 2458–2462, 2009.

[39] T. Salmi, *et al*.,"A novel computer code for modeling quench protection heaters in high-field $Nb_3Sn$ accelerator magnets," *IEEE Trans. Appl. Supercond.*, 24 4, 2014.

[40] G. Ambrosio, *et al*.," Test Results of the First 3.7 m Long Nb3Sn Quadrupole by LARP and Future Plans" *IEEE Trans. Appl. Supercond.*, 21 3, 1858-1862, 2011.